

# Improvement of Metal-Semiconductor Contact from Schottky to Ohmic by Cu Doping in Transition Metal Dichalcogenide Transistors

Maomao Liu,<sup>1</sup> Simran Shahi,<sup>1</sup> Sara Fathipour,<sup>2</sup> Wansik Hwang,<sup>3</sup> Maja Remskar,<sup>4</sup> Alan Seabaugh,<sup>2</sup> and Huamin Li<sup>1</sup>

<sup>1</sup>Department of Electrical Engineering, University at Buffalo, the State University of New York, Buffalo, USA

<sup>2</sup>Department of Electrical Engineering, University of Notre Dame, Indiana, USA

<sup>3</sup>Department of Materials Engineering, Korea Aerospace University, Goyang, Korea

<sup>4</sup>Solid State Physics Department, Jozef Stefan Institute, Ljubljana, Slovenia

Email: seabaugh.l@nd.edu, huaminli@buffalo.edu

**Abstract**—Metal-semiconductor (MS) contacts were changed from Schottky to Ohmic in synthesized tungsten disulfide (WS<sub>2</sub>), due to Cu doping during the synthesis. Significant reductions of contact barrier and resistance were achieved. A statistical study shows transistor performance including carrier mobilities, on/off ratios, on-current densities, and subthreshold swings were also improved significantly with Cu doping.

## I. INTRODUCTION

Two-dimensional (2D) layered crystals such as transition metal dichalcogenides (TMDs) have strong in-plane covalent bonding and weak out-of-plane van der Waals (vdW) interaction. Theoretical models predict that among various semiconducting TMDs, WS<sub>2</sub> has the highest electron mobility and the best transistor performance including the highest on/off ratios and on-current densities [1, 2]. However, to apply WS<sub>2</sub> into complementary metal-oxide-semiconductor logic circuits, contact engineering is highly required [3-5]. In this work, we report significantly improved performance of few-layer WS<sub>2</sub> field-effect transistors (FETs) by Cu doping. Compared to pristine-WS<sub>2</sub> FETs, the Cu-doped WS<sub>2</sub> (Cu-WS<sub>2</sub>) devices show a notable reduction of MS barrier height and contact resistance, and a Schottky-to-Ohmic contact improvement. Transistor performance, including carrier mobilities ( $\mu_{FE}$ ), on/off ratios, on-current densities ( $J_{D,on}$ ), subthreshold swings (SS) were also improved considerably based on a statistical study. This work has demonstrated the potential of metal doping for 2D material engineering and device applications.

## II. MATERIAL SYNTHESIS AND DEVICE FABRICATION

Both pristine-WS<sub>2</sub> and Cu-WS<sub>2</sub> are synthesized by chemical transport reaction in a two-zone oven, as shown in Fig. 1. The pristine-WS<sub>2</sub> uses S and W as sources; in contrast, the Cu-WS<sub>2</sub> has 0.5 wt. % of Cu foil in addition to S and W sources. The transport reaction runs at 1060 K in an evacuated silica ampoule at a pressure of 10<sup>-2</sup> Pa and with a temperature gradient of 5.6 K/cm. Cu forms compounds CuI and is transported to the colder side of the ampoule. After 21 days of growth the silica ampoule was slowly cooled to room temperature with a controlled cooling rate of 30 °C per hour.

After synthesis, the flakes are mechanically exfoliated and transferred onto a Si substrate which has a 90-nm-thick SiO<sub>2</sub>.

The source and drain electrodes, Ti (10 nm)/Au (100 nm), are patterned by electron beam lithography and deposited by electron beam evaporation. All the devices have the channel length ( $L$ ) of 1  $\mu$ m and various channel widths ( $W$ ). The measurements are performed in a dark N<sub>2</sub> ambient. Drain current ( $I_D$ ) is measured at various drain voltages ( $V_D$ ) and back-gate voltages ( $V_{BG}$ ), and normalized to obtain drain current density ( $J_D=I_D/W$ ) for comparison.

## III. RESULTS AND DISCUSSION

Raman spectra (488 nm, 1.5 mW) for both pristine-WS<sub>2</sub> and Cu-WS<sub>2</sub> samples indicate two peaks: in-plane vibration ( $E^{1_{2g}}$ ) peak at  $\sim 357$  cm<sup>-1</sup> and out-of-plane vibration ( $A_{1g}$ ) peak at  $\sim 423$  cm<sup>-1</sup>, as shown in Fig. 2 (a). No peak shift is detected with Cu doping, indicating that the physical structure of WS<sub>2</sub> is not affected by Cu doping in the van der Waals (vdW) gaps. Both the peak intensity ratios ( $E^{1_{2g}}/A_{1g} < 1$ ) suggest few-layer structures, which are also confirmed by atomic force microscope (AFM). The flake thickness is  $\sim 4$  nm for the pristine-WS<sub>2</sub> FET and  $\sim 6$  nm for Cu-WS<sub>2</sub> FET, as shown in Fig. 2 (b).

Output characteristics ( $J_D-V_D$ ) and transfer characteristics ( $J_D-V_{BG}$ ) of pristine-WS<sub>2</sub> FET are shown in Fig. 3. At room temperature, pristine-WS<sub>2</sub> is n-type doped and shows electron transport. A non-linear  $I-V$  relation at small  $V_D$  indicates a Schottky contact between Ti and pristine-WS<sub>2</sub>. The lowest SS and highest  $\mu_{FE}$  are 2.3 V/dec and 4.9 cm<sup>2</sup>/Vs, respectively. According to the hysteresis of charge neutral point ( $\Delta V_{CNP}$ ), the effective trap density ( $n_t$ ) is estimated as  $n_t = C_{ox} \cdot \Delta V_{CNP} / q = 3.1 \times 10^{12}$  cm<sup>-2</sup>, where  $C_{ox}$  is the oxide capacitance ( $3.83 \times 10^{-8}$  F/cm<sup>2</sup>), and  $q$  is the electronic charge. As a comparison,  $J_D-V_D$  and  $J_D-V_{BG}$  of Cu-WS<sub>2</sub> FET are shown in Fig. 4. The linear  $I-V$  relation at small  $V_D$  suggests an Ohmic contact between Ti and Cu-WS<sub>2</sub>, which is significantly improved compared to pristine-WS<sub>2</sub>. Moreover, the Cu-WS<sub>2</sub> FET shows a clear current saturation at large  $V_D$ , which is not seen in pristine-WS<sub>2</sub> FET. The lowest SS, highest  $\mu_{FE}$ , and  $n_t$  of Cu-WS<sub>2</sub> FET are obtained as 2.4 V/dec, 21.9 cm<sup>2</sup>/Vs, and  $3.4 \times 10^{12}$  cm<sup>-2</sup>, respectively.

Temperature-dependent electronic transport is investigated in the temperature ( $T$ ) range from 218 to 298 K. Transconductance ( $g_m$ ) as a function of  $V_{BG}$  for pristine-WS<sub>2</sub> FET is shown in Fig. 5 (a). A crossover from an insulating regime

(increase of  $g_m$  with increasing  $T$ ) to a metallic regime (decrease of  $g_m$  with increasing  $T$ ) is observed at around at  $\sim 10$  V. This metal-insulator transition (MIT) point corresponds to 2D carrier density ( $n_{2D} = C_{ox} \cdot V_{BG}/q$ ) of  $2.4 \times 10^{12} \text{ cm}^{-2}$ , and it is the direct consequence of quantum interference effects (QIEs) of weak localization at low carrier densities ( $V_{BG} < 10$  V) and strong localization at high carrier densities ( $V_{BG} > 10$  V) [2]. Similar MIT behavior has also been found in MoS<sub>2</sub> devices [6]. Activation energy ( $E_a$ ) is estimated by fitting  $g_m$  with the expression  $g_m = g_{m0} \cdot \exp[-E_a/(k_B T)]$ , as shown in Fig. 5 (b), where  $g_{m0}$  is a constant, and  $k_B$  is the Boltzmann constant. The  $E_a$  corresponds to the thermal activation of charge carriers at the Fermi energy into the conduction band, and its dependence on  $V_{BG}$  can be used to extract the density of states (DOS) as  $(dV_{BG}/dE_a - 1) \cdot C_{ox}/q^2$ . The maximum DOS is on the order of  $10^{14} \text{ eV}^{-1} \text{ cm}^{-2}$ , which is consistent with the theoretical calculation ( $2.85 \times 10^{14} \text{ eV}^{-1} \text{ cm}^{-2}$ ) [2], as shown in Fig. 5 (c). The MS barrier height ( $\phi_{MS}$ ) is also estimated based on a thermal emission dominated  $I$ - $V$  relation as  $J_D \propto T^2 \cdot \exp[-\phi_{MS}/(k_B T)]$  assuming  $\exp[-qV_D/(k_B T)] \ll 1$  [7], as shown in Fig. 5 (d). Both the  $E_a$  and  $\phi_{MS}$  are consistent with each other, suggesting that the carrier transport is limited by the MS contact. As a comparison, Cu-WS<sub>2</sub> FET shows the MIT transition at  $\sim 5$  V, which corresponds to  $n_{2D}$  of  $1.2 \times 10^{12} \text{ cm}^{-2}$ , as shown in Fig. 6. The maximum DOS is also on the order of  $10^{14} \text{ eV}^{-1} \text{ cm}^{-2}$ . In the insulating regimes, the maximum  $E_a$  and  $\phi_{MS}$  in Cu-WS<sub>2</sub> is about  $\sim 300$  meV, which is less than pristine-WS<sub>2</sub> ( $\sim 400$  meV). This reduced MS barrier height interprets the improvement of contact condition from Schottky to Ohmic by Cu doping.

To further investigate the impact of Cu doping on MS contacts, energy band diagrams are illustrated in Fig. 7. Both the few-layer pristine-WS<sub>2</sub> and Cu-WS<sub>2</sub> have the bandgap ( $E_g$ ) of  $\sim 1.3$  eV and the electron affinity ( $\chi$ ) of 3.9 eV [8]. The workfunction ( $\phi_S$ ) is estimated as  $\sim 4.3$  eV for pristine-WS<sub>2</sub> and  $\sim 4.1$  eV for Cu-WS<sub>2</sub>. The smaller  $\phi_S$  in Cu-WS<sub>2</sub> is due to the electron transfer and chemical interaction between Cu and chalcogenide layers, which increases the Fermi energy and carrier density [3-5]. Due to a gate-controlled Schottky barrier modulation in TMDs [9, 10],  $\phi_{MS}$  depends linearly on  $V_{BG}$  when  $V_{BG}$  is smaller than the flatband voltage ( $V_{FB}$ ), and the charge injection through the barrier is dominated by thermionic emission. When  $V_{BG}$  is larger than  $V_{FB}$ ,  $\phi_{MS}$  should not change with  $V_{BG}$  and thus deviates from this linear relation. The charge injection in this region is dominated both thermionic emission and Fowler-Nordheim (F-N) tunneling [6], and the further decrease of  $\phi_{MS}$  value is due to the thinning of Schottky barrier. The  $\phi_{MS}$  at  $V_{FB}$  ( $\phi_{MS0}$ ) for both pristine-WS<sub>2</sub> and Cu-WS<sub>2</sub> are extracted at the point where  $\phi_{MS}$  stops depending linearly on  $V_{BG}$ , as shown in Fig. 8. It is also noted that a Schottky barrier lowering occurs with the increasing  $V_D$  due to an image-forces-induced underestimation of  $\phi_{MS0}$ . This can be eliminated by plotting  $\phi_{MS0}$  as a function of  $V_D$  and then extracting  $\phi_{MS0}$  at zero  $V_D$  by a linear extrapolating [7]. The  $\phi_{MS0}$  is 116 and 92 meV for pristine-WS<sub>2</sub> and Cu-WS<sub>2</sub>, respectively. These values are smaller than the results from density functional theory (DFT) calculation for 1L-WS<sub>2</sub> [11], due to the much larger  $E_g$  ( $\sim 2.1$  eV) of single layer form.

Temperature-dependent  $\mu_{FE}$  in Cu-WS<sub>2</sub> FET is extracted from  $g_m$ , which is about 5 times higher than pristine-WS<sub>2</sub>, as shown in Fig. 9. The dependence of  $\mu_{FE}$  on  $T$  follows a power-law as  $\mu_{FE} \propto T^\kappa$ . The temperature damping factor  $\kappa$  is 0.72 for pristine-WS<sub>2</sub> and 0.70 for Cu-WS<sub>2</sub>, suggesting that the Cu doping has negligible effect on charge impurity scattering or screening [2].

Contact resistance ( $R_c$ ) is extracted from a combination of two-contact and four-contact measurements, as shown in Fig. 10. Compared to pristine-WS<sub>2</sub>,  $R_c$  in Cu-WS<sub>2</sub> is about 3 orders of magnitude lower at low carrier densities ( $V_{BG} = 10$  V), and about 1 order lower at high carrier densities ( $V_{BG} = 30$  V). Besides, channel resistivity ( $\rho_{channel}^{2D} = R_{ch} \cdot W/L$ ) is also obtained, which is superior to 1L-WS<sub>2</sub> and comparable with chemically doped few-layer WS<sub>2</sub> [7].

A statistical study of transistor performance is carried out for 26 pristine-WS<sub>2</sub> FETs and 29 Cu-WS<sub>2</sub> FETs, as shown in Fig. 11. Due to the Cu doping, the mean values of  $\mu_{FE}$ , on/off ratios, and  $J_{D,on}$  are about 5, 4 and 2 times increased, respectively; the mean SS is over 30% decreased.

#### IV. CONCLUSION

The significant improvement of MS contact from Schottky to Ohmic in WS<sub>2</sub> FETs was obtained by Cu doping. The average carrier mobilities, on-current densities, on/off ratios, etc. were all increased to 10.1 cm<sup>2</sup>/Vs, 1.2  $\mu\text{A}/\mu\text{m}$ , and  $2.5 \times 10^6$ , respectively.

#### REFERENCES

- [1] L. Liu, S. B. Kumar, Y. Ouyang, and J. Guo, "Performance limits of monolayer transition metal dichalcogenide transistors," *IEEE Trans. Electron Dev.*, vol. 58, pp. 3042-3047, 2011.
- [2] D. Ovchinnikov, A. Allain, Y.-S. Huang, D. Dumcenco, and A. Kis, "Electrical transport properties of single-layer WS<sub>2</sub>," *ACS Nano*, vol. 8, pp. 8174-8181, 2014.
- [3] H. Wang, H. Yuan, S. S. Hong, Y. Li, and Y. Cui, "Physical and chemical tuning of two-dimensional transition metal dichalcogenides," *Chem. Soc. Rev.*, vol. 44, pp. 2664-2680, 2015.
- [4] D. S. Schulman, A. J. Arnold, and S. Das, "Contact engineering for 2D materials and devices," *Chem. Soc. Rev.*, vol. 47, pp. 3037-3058, 2018.
- [5] Y. Zhao, K. Xu, F. Pan, C. Zhou, F. Zhou, and Y. Chai, "Doping, contact and interface engineering of two-dimensional layered transition metal dichalcogenides transistors," *Adv. Funct. Mater.*, vol. 27, no. 1603484, 2016.
- [6] B. Radisavljevic, and A. Kis, "Mobility engineering and a metal-insulator transition in monolayer MoS<sub>2</sub>," *Nat. Mater.*, vol. 12, pp. 815-820, 2013.
- [7] A. Allain, J. Kang, K. Banerjee, and A. Kis, "Electrical contacts to two-dimensional semiconductors," *Nat. Mater.*, vol. 14, pp. 1195-1205, 2015.
- [8] J. Kang, S. Tongay, J. Zhou, J. Li, and J. Wu, "Band offsets and heterostructures of two-dimensional semiconductors," *Appl. Phys. Lett.*, vol. 102, no. 012111, 2013.
- [9] H.-M. Li, D.-Y. Lee, M.-S. Choi, D.-S. Qu, X.-C. Liu, C.-H. Ra, and W. J. Yoo, "Gate-controlled Schottky barrier modulation for superior photoresponse of MoS<sub>2</sub> field effect transistors," in *IEEE IEDM Tech. Dig.*, pp. 507-510, 2013.
- [10] H.-M. Li, D.-Y. Lee, M.-S. Choi, D. Qu, X. Liu, C.-H. Ra, and W. J. Yoo, "Metal-semiconductor barrier modulation for high photoresponse in transition metal dichalcogenide field effect transistors," *Sci. Rep.*, vol. 4, no. 4041, 2014.
- [11] Y. Guo, D. Liu, and J. Robertson, "3D behavior of Schottky barriers of 2D transition-metal dichalcogenides," *ACS Appl. Mater. Interfaces*, vol. 7, pp. 25709-25715, 2015.

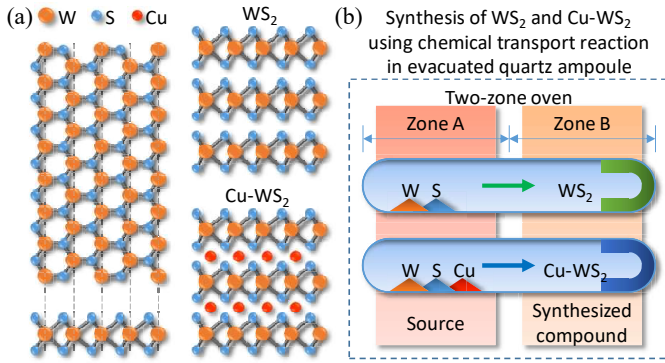


Fig. 1. (a) Atomic structure of WS<sub>2</sub> and Cu-WS<sub>2</sub>. (b) Schematic of material synthesis using chemical transport reaction.

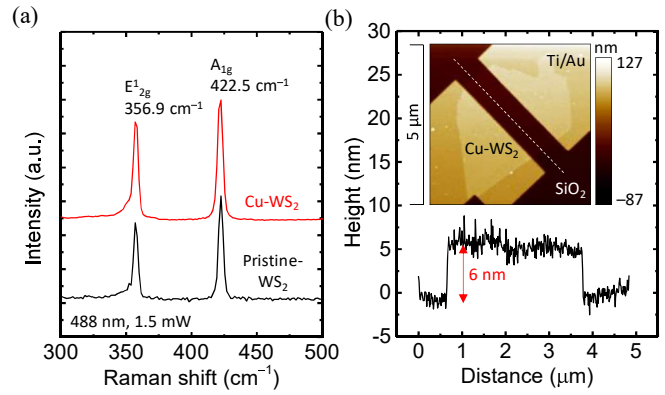


Fig. 2. (a) Raman spectrum of few-layer pristine-WS<sub>2</sub> and Cu-WS<sub>2</sub>. (b) AFM characterization of a few-layer Cu-WS<sub>2</sub> FET.

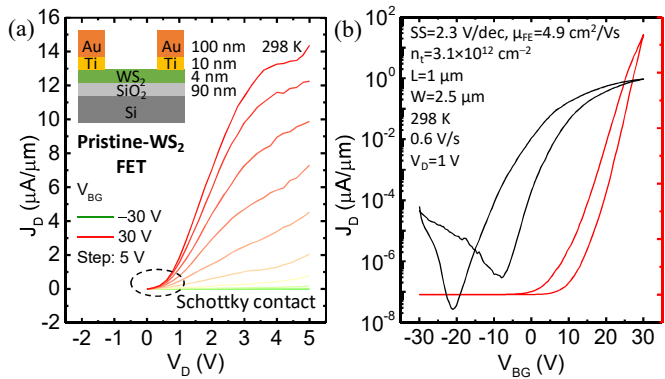


Fig. 3. (a)  $J_D$ - $V_D$  and (b)  $J_D$ - $V_{BG}$  characteristics of pristine-WS<sub>2</sub> FET at room temperature.

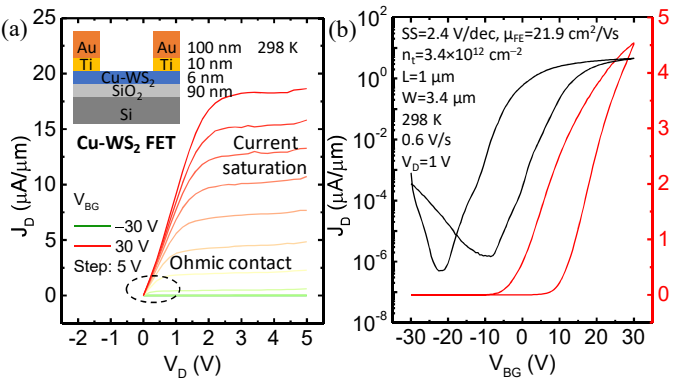


Fig. 4. (a)  $J_D$ - $V_D$  and (b)  $J_D$ - $V_{BG}$  characteristics of Cu-WS<sub>2</sub> FET at room temperature.

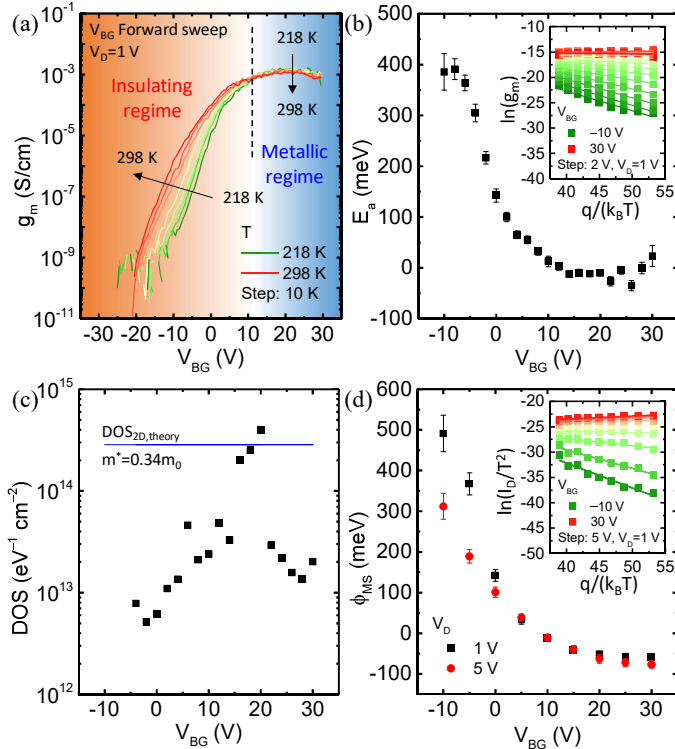


Fig. 5. (a)  $g_m$ , (b)  $E_a$ , (c) DOS, and (d)  $\phi_{MS}$  as functions of  $V_{BG}$  in pristine-WS<sub>2</sub> FET.

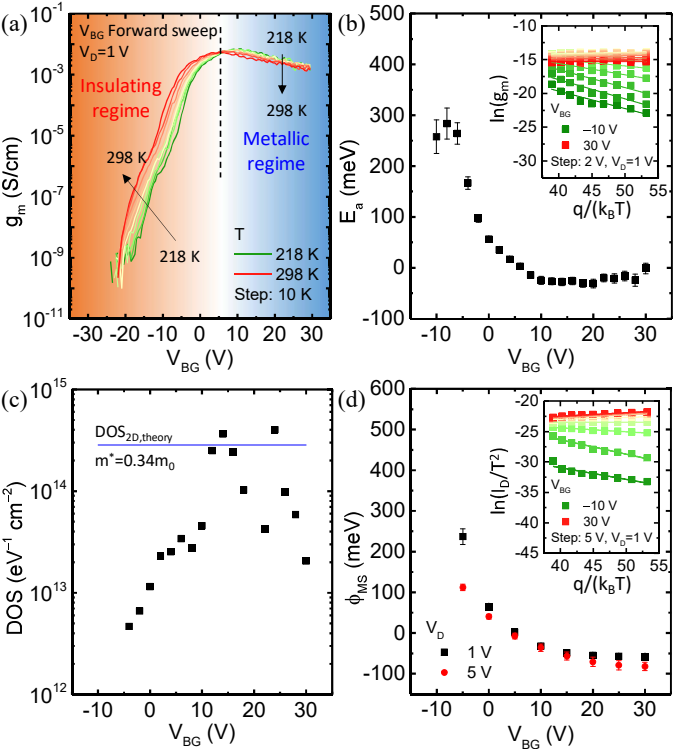


Fig. 6. (a)  $g_m$ , (b)  $E_a$ , (c) DOS, and (d)  $\phi_{MS}$  as functions of  $V_{BG}$  in Cu-WS<sub>2</sub> FET.

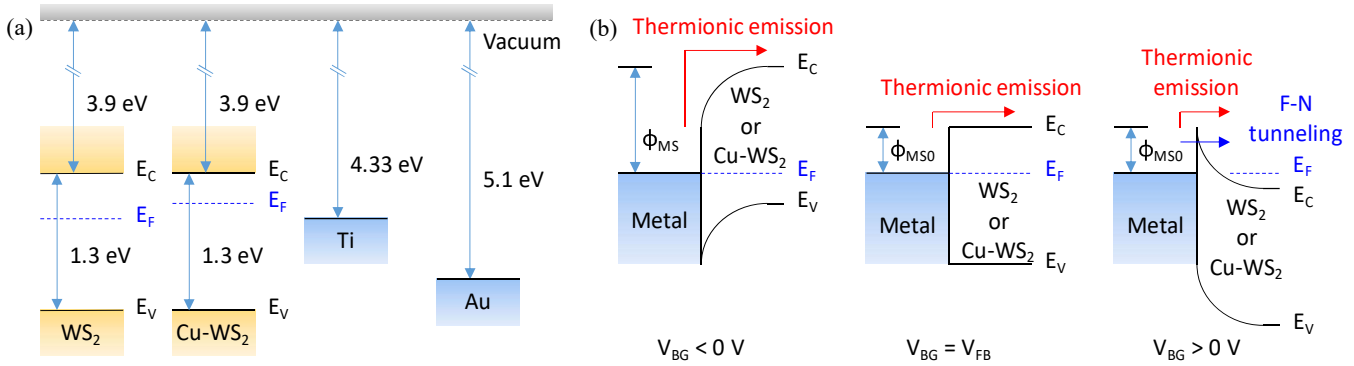


Fig. 7. (a) Energy band diagram of pristine-WS<sub>2</sub>, Cu-WS<sub>2</sub>, Ti, and Au. (b) MS contact barriers at different  $V_{BG}$ , including  $V_{BG} < 0$  V,  $V_{BG} = V_{FB}$ , and  $V_{BG} > 0$  V. Here  $E_F$  is the Fermi energy level,  $E_C$  and  $E_V$  are conduction band and valence band, respectively.

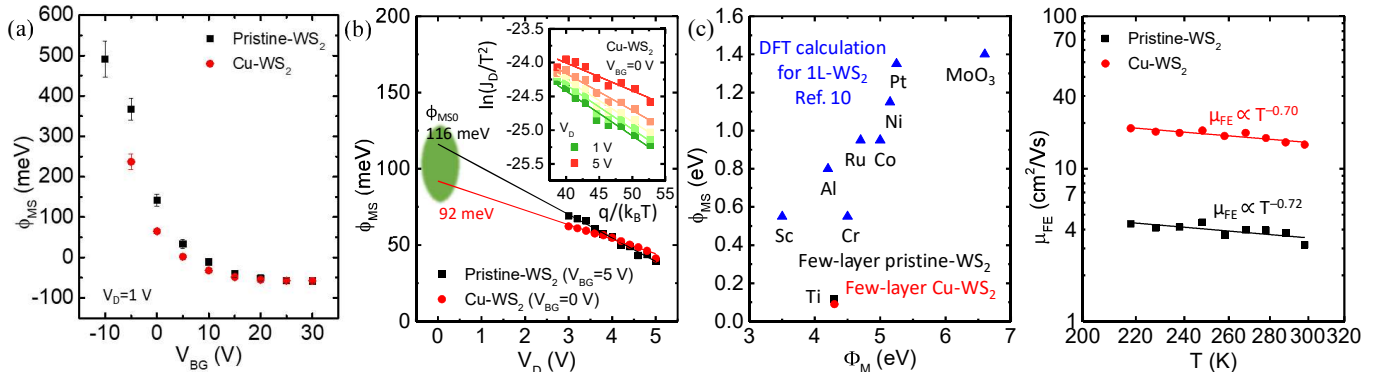


Fig. 8. (a)  $\phi_{MS}$  as a function of  $V_{BG}$  for extracting  $\phi_{MS0}$  at  $V_{FB}$ . (b)  $\phi_{MS0}$  as a function of  $V_D$  for eliminating barrier lowering at finite  $V_D$ . (c) Comparison of  $\phi_{MS}$  for various metal workfunctions ( $\phi_M$ ).

Fig. 9.  $\mu_{FE}$  as a function of  $T$  fitted by a power-law relation.

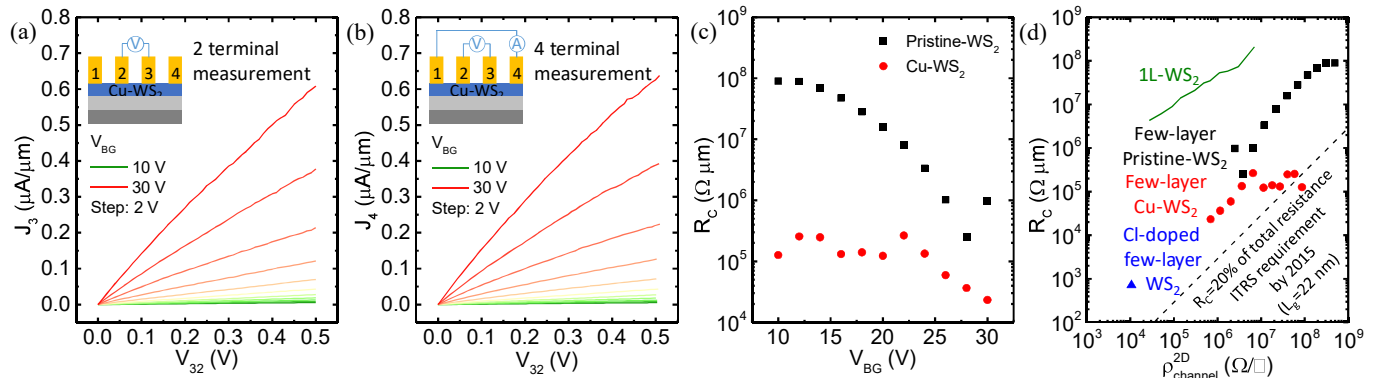


Fig. 10. (a)  $I$ - $V$  relation of Cu-WS<sub>2</sub> FET in 2 terminal measurement. (b)  $I$ - $V$  relation of Cu-WS<sub>2</sub> FET in 4 terminal measurement. (c) Calculated  $R_c$  as a function of  $V_{BG}$ . (d)  $R_c$  as a function of  $\rho_{\text{channel}}^{2D}$  for 1L-WS<sub>2</sub>, few-layer WS<sub>2</sub> and chemically doped WS<sub>2</sub>.

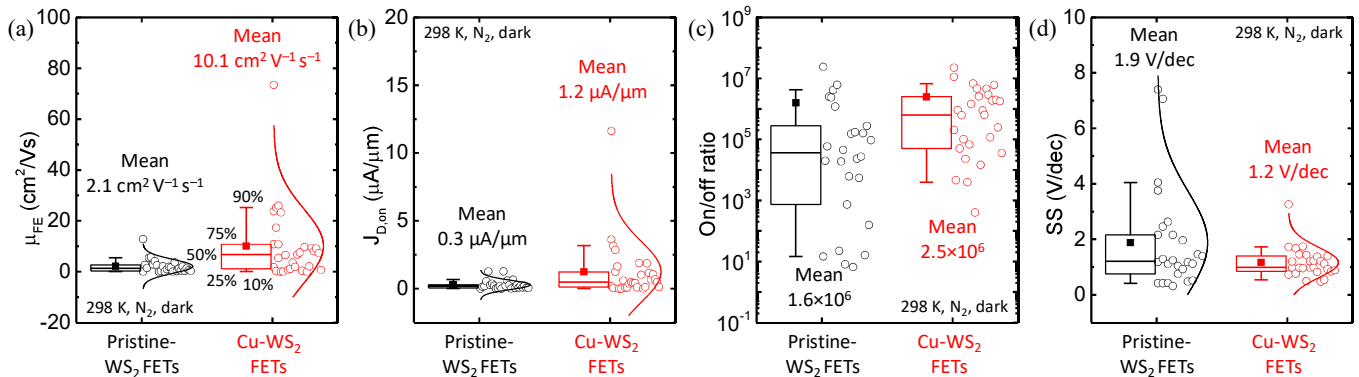


Fig. 11. A statistical study of transistor performance comparison for 26 pristine-WS<sub>2</sub> FETs and 29 Cu-WS<sub>2</sub> FETs, including (a)  $\mu_{FE}$ , (b) on/off ratios, (c)  $J_{D, on}$ , and (d) SS.